Contribution from the Department of Chemistry,
Miami University, Oxford, Ohio 45056

Iron(III)-Catalyzed Decomposition of the Chlorite Ion: An Inorganic Application of the Quenched Stopped-Flow Method

István Fábián† and Gilbert Gordon*

Received July 30, 1991

The kinetics and mechanism of the iron(III)-catalyzed decomposition of the chlorite ion have been investigated by using conventional batch, stopped-flow, stopped-flow–rapid-scan spectrophotometric, and quenched stopped-flow methods at 25 °C and in 1.0 M $NaClO_4$. The concentration vs time profiles were determined for chlorite ion, chlorine dioxide, and, in a few cases, chloride ion in the 40 ms–several minute interval. It was confirmed that the stoichiometry can be given as the appropriate combination of the following reactions: $4HClO_2 = 2ClO_2 + ClO_3^- + Cl^- + 2H^+ + H_2O$; $5HClO_2 = 4ClO_2 + Cl^- + H^+ + 2H_2O$. The proposed mechanism postulates that the catalytic decomposition is initiated by the formation of the $FeClO_2^{2+}$ complex and the rate-determining step is the redox decomposition of this species. The mechanism was validated by model calculations based on the GEAR algorithm. The measured and calculated kinetic curves are in excellent agreement under a variety of experimental conditions. It was shown that the overall stoichiometry is kinetically controlled and ultimately determined by fast secondary reactions between various chlorine species. This work represents the first totally inorganic application of the quenched stopped-flow method. Several aspects of this technique are discussed.

Introduction

In aqueous solution, the disproportionation of the chlorite ion[1] exhibits complex stoichiometric and kinetic patterns.[2] The stoichiometry is kinetically controlled[3] and can be expressed as a linear combination of eqs 1 and 2.

$$4HClO_2 = 2ClO_2 + ClO_3^- + Cl^- + 2H^+ + H_2O \quad (1)$$

$$5HClO_2 = 4ClO_2 + Cl^- + H^+ + 2H_2O \quad (2)$$

The rate of disproportionation is significantly enhanced by various inorganic and organic species. This was frequently utilized in chlorite ion based oscillation reactions[4] or in other systems showing exotic kinetic phenomena.[5]

Ferric ion catalyzes the ClO_2^- decomposition.[6-8] On the basis of spectrophotometric experiments, Schmitz and Rooze[8] reported the stoichiometry to be consistent with reaction 1 and concluded that the reaction order with respect to chlorite ion, ferric ion, and chlorine dioxide is 2, 1, and −1, respectively.

Recently, we have investigated the same system in the sub-second region by using stopped-flow (SF) and stopped-flow–rapid-scan spectrophotometric (SF-RS) methods. The formation[9] of $FeClO_2^{2+}$ (K = 13.8 M^{-1}) was found to be fast and kinetically coupled with the decomposition of the chlorite ion. Chlorine dioxide formation was observed in significant amounts in a few hundred milliseconds after mixing the reactants. The formation of the $FeClO_2^{2+}$ complex, which is not included in the Schmitz and Rooze mechanism, as well as the fast initial steps is of crucial kinetic importance in the overall mechanism.

In this study, the kinetics of the iron(III)-catalyzed chlorite ion decomposition were investigated by using a combination of conventional batch, SF, SF-RS, and quenched stopped-flow (QSF) experiments. This appears to be the first totally inorganic application of the QSF method.[10] It provides direct information for the concentration vs time profiles of the reactants and products in the sub-second time domain. These data and our recent results[9] can serve to develop and verify a detailed mechanism for the decomposition of ClO_2^- under a wide range of experimental conditions. At the same time, we expect that the results will contribute to our understanding of the chemistry of the chlorite ion.

Experimental Section

Chemicals. The recrystallization of $NaClO_2$ from commercially available sodium chlorite (OLIN; approximately 80% purity) and the preparation of the iron(III) stock solutions were described earlier.[9,11,12] Chloroacetic acid was twice recrystallized from 95% ethanol. All other chemicals, sodium fluoride and formate (Matheson Coleman & Bell) and sodium acetate and perchloric acid (Fisher), were of the highest commercially available grade and were used without further purification.

The concentrations of ClO_2^-, Fe^{3+}, and the pH were varied in the ranges 0.001–0.25 M, 5.0×10^{-5}–5.0×10^{-3} M, and 1.0–4.5, respectively. The ionic strength was adjusted to 1.0 M with sodium perchlorate prepared from Na_2CO_3 (Fisher) and $HClO_4$. The temperature was set at 25.0 ± 0.05 °C in all experiments.

Conventional Kinetic Measurements. The reaction was triggered by adding small aliquots of acidic Fe^{3+} solution to vigorously stirred ClO_2^- solutions. The reaction mixture was immediately transferred into a tightly sealed cuvette, and the spectra were recorded on a Hewlett Packard 8450 UV–visible diode array spectrophotometer. Measurements were made in both the presence and the absence of acetate, formate, or chloroacetate buffer. The pH of the samples was either calculated on the basis of the appropriate equilibrium data (pH <2.3) or measured with a Radiometer GK2401B combination glass electrode attached to a Radiometer PHM64 pH meter. The electrode was calibrated such that the pH-meter reading directly gave the hydrogen ion concentration (−log $[H^+]$).

Stopped-Flow Measurements. The reaction was followed with an Atago Bussan/Photal Otsuka Electronics RA-401 stopped-flow instrument attached to an RA-451 data processor unit. The SF and SF-RS traces were monitored with a Hamamatsu R374 photomultiplier and a 512-channel diode array detector, respectively. The SF traces were taken as the average of at least five replicate runs. In these experiments, the base line was set to 0.0 absorbance with 1.0 M $NaClO_4$; thus, the results can be compared directly to other spectrophotometric data.

Stoichiometry. At various reaction times, 25-cm^3 aliquots of the reaction mixture were mixed with 1 cm^3 of 0.5 M NaF solution and the pH was set between 3.3 and 3.7 by adding appropriate amounts of chloroacetate buffer. Thus, iron(III) was completely converted into catalytically inactive fluoro complexes and the decomposition was stopped. Since the final pH was relatively high, the uncatalyzed decomposition of the chlorite ion was also quenched. In a carefully sealed cuvette, the spectra of the samples did not change over more than 15–20 min.

†On leave from the Institute of Inorganic and Analytical Chemistry, Kossuth L. University, Debrecen, Hungary.

(1) Chlorite ion and chlorous acid are in fast acid–base equilibria and are present in a concentration ratio determined by the actual pH. In this paper, the two species will be distinguished only when it is required for the clarity of the presentation.

(2) Gordon, G.; Kieffer, R. G.; Rosenblatt, D. H. In *Progress in Inorganic Chemistry*; Lippard, S. J., Ed.; Wiley-Interscience: New York, 1972; Vol. 15, pp 201–286.
(3) Kieffer, R. G.; Gordon, G. *Inorg. Chem.* **1968**, *7*, 235.
(4) Epstein, I. R.; Orbán, M. In *Oscillations and Traveling Waves in Chemical Systems*; Field, R. J., Burger, M., Eds.; Wiley: New York, 1985; pp 257–286.
(5) De Kepper, P.; Boissonade, J.; Epstein, I. R. *J. Phys. Chem.* **1990**, *94*, 6525 and references therein.
(6) Launer, H. F.; Wilson, W. K.; Flynn, J. H. *J. Res. Natl. Bur. Stand.* **1953**, *51*, 237.
(7) Launer, H. F.; Tomimatsu, Y. *J. Am. Chem. Soc.* **1954**, *76*, 2591.
(8) Schmitz, G.; Rooze, H. *Can. J. Chem.* **1984**, *62*, 2231; **1985**, *63*, 976.
(9) Fábián, I.; Gordon, G. *Inorg. Chem.* **1991**, *30*, 3994.
(10) Simándi, L.; Jáky, M. *J. Am. Chem. Soc.* **1976**, *98*, 1995.
(11) Peintler, G.; Nagypál, I.; Epstein, I. R. *J. Phys. Chem.* **1990**, *94*, 2954.
(12) Fábián, I.; Gordon, G. *Inorg. Chem.* **1991**, *30*, 3785.

0020-1669/92/1331-2144$03.00/0 © 1992 American Chemical Society

Table I. Typical Stoichiometric Results from Conventional Kinetic Studies for the Iron(III)-Catalyzed Chlorite Ion Decomposition[a]

time, min	$10^3C_{ClO_2^-}$, M	$10^3C_{ClO_2}$, M	$10^3C_{Cl^-}$, M	$\Delta C_{ClO_2^-}/C_{ClO_2}$	C_{ClO_2}/C_{Cl^-}	av oxidn no.[b]
0.0	10.42					3.00
0.5	8.12	1.34	0.52	1.72	2.53	3.01
1.0	7.53	1.66	0.71	1.74	2.32	2.98
2.0		2.17	0.96		2.25	
4.0	6.20	2.44	1.08	1.73	2.27	2.96
10.0	4.76	3.20	1.40	1.77	2.28	2.97
15.0	4.12	3.52	1.55	1.79	2.28	2.99
20.0	3.64	3.69	1.62	1.73	2.28	3.01
30.0	3.05	3.91	1.81	1.88	2.16	3.00
45.0	2.39	4.21	1.95	1.90	2.16	3.02

[a] Conditions: $C_{ClO_2^-} = 1.04 \times 10^{-2}$ M, $C_{Fe^{3+}} = 8.52 \times 10^{-4}$ M, $C_{HCOONa} = 0.040$ M, $C_{HClO_4} = 0.030$ M. [b] Average oxidation number $= (3C_{ClO_2^-} + 4C_{ClO_2} + 5C_{ClO_3^-} - C_{Cl^-})/C^0_{ClO_2^-}$.

This time interval was sufficiently long to analyze the reaction mixture by various methods.

Fluoride ion forms very stable nonabsorbing complexes with iron(III),[13,14] and the concentrations of ClO_2^- and ClO_2 could be determined without interference by using the HP spectrophotometer. In a few cases, the total concentration of these two species was determined by using an iodometric method[15] in order to verify the spectrophotometric results. The titrations were made with a Radiometer ABU93 Triburette autoburette station which was connected to a Radiometer VIT90 Video Titrator unit equipped with a standard P101 platinum–K401 SCE electrode pair (Radiometer).

The chloride ion concentration was determined by potentiometric titrations with 0.002 M $AgNO_3$ solution in 70% methanol using a P101 platinum–F1012Cl chloride ion selective electrode pair (Radiometer).[16] Because of the relatively low concentration levels of chloride ion, the ±2.0% error of these titrations was higher than usual. The difference between the concentration of initially added ClO_2^- and the sum of the concentrations of ClO_2, ClO_2^-, and Cl^- was attributed to the chlorate ion. On the basis of this assumption, the calculated average oxidation number is in excellent agreement with the theoretical value of 3 (cf. Table I). This confirms that other chlorine species and/or oxygen is not formed in significant concentrations.

Quenched Stopped-Flow Experiments. The QSF measurements were made with a Hi-Tech Scientific Model PQ-53 Preparative Quencher. The basic concepts of this method and the details of the experiments will be discussed in the next section.

Results

Kinetic runs without added iron(III) confirmed that the contribution of the uncatalyzed pathway to the overall decomposition of chlorite ion sharply decreases by increasing the pH. The importance of the uncatalyzed pathway was found to be minimal even at the lowest pH and iron(III) concentrations applied in this study.

Figure 1 shows the typical spectral change observed in the presence of the catalyst. The absorbance increase at 360 nm is primarily attributed to chlorine dioxide formation. In the 230–280-nm region, the net effect of the disappearance of chlorite ion and the formation of ClO_2 is observed. In particular, in the far-UV region, various iron species also may have some contribution to the observed spectra.[17,18] The spectral changes indicate that, after a relatively fast initiation period, the decomposition markedly slows down.

The same general kinetic profile was found under a variety of experimental conditions. However, in the presence of buffers, the decomposition rate decreases. This is most likely the result of complex formation between iron(III) and the buffer, which decreases the concentration of the catalytically active iron species.

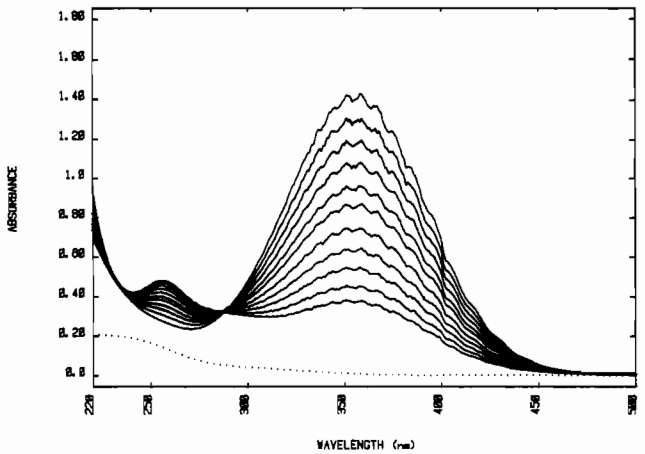

Figure 1. Typical absorption spectra for the iron(III)-catalyzed decomposition of chlorite ion as a function of time (0.5-cm cell). $C_{ClO_2^-} = 5.20 \times 10^{-3}$ M, $C_{Fe^{3+}} = 1.10 \times 10^{-3}$ M, and pH = 2.40. In the order of increasing absorbance at 360 nm, the spectra were recorded 20, 30, 50, 80, 140, 240, 360, 600, 1000, 1800, and 4000 s after mixing the reactants. Dotted line: spectrum of Fe(III) at the same pH.

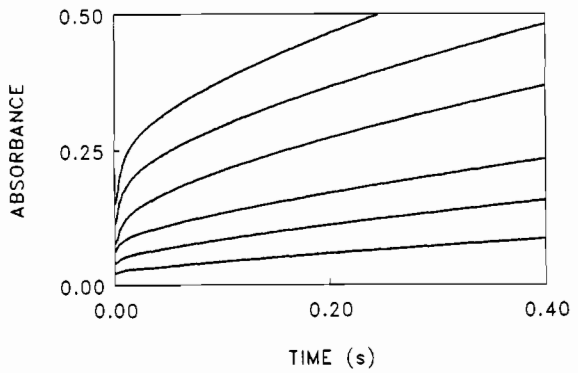

Figure 2. Selected stopped-flow traces recorded in a 10-mm cell for the iron(III)-catalyzed decomposition of chlorite ion at 370 nm. $C_{ClO_2^-} = 9.93 \times 10^{-3}$ M and $C_{HClO_4} = 6.67 \times 10^{-3}$ M. In increasing order of the absorbance, $C_{Fe^{3+}}$ for these curves is 5.51×10^{-5}, 1.38×10^{-4}, 2.75×10^{-4}, 5.51×10^{-4}, 8.26×10^{-4}, and 1.10×10^{-3} M.

In acetate, formate, or chloroacetate buffer, the decay of the reaction rate by increasing pH shows good correlation with the formation of the corresponding iron(III) monocomplex.[13]

In the absence of buffers, the decomposition rate varies only slightly with pH in the 1.0–2.3 region. However, at higher pH values and at longer reaction times, the absorbance slowly decreases in the 360-nm region. Also, larger than expected absorbance changes are observed around the 260-nm maximum of the chlorite ion. These spectral observations are attributed to hydrolytic reactions of iron(III). The formation of polynuclear iron species is typically associated with slow spectral changes in the UV region.[17]

Chloride ion strongly affects both the stoichiometry and kinetics of the uncatalyzed disproportionation of chlorite ion.[3,19] In the present study, replicate kinetic runs were carried out by varying chloride ion concentrations up to 0.1 M. The corresponding near-UV–visible spectra were identical within the experimental limitations. However, in the far-UV region, the absorbance invariably was slightly higher in the presence of chloride ion. The observed deviations are consistent with the formation of strongly absorbing iron(III) chloro complexes at low concentration levels. These measurements also confirmed that the product chloride ion has at most marginal kinetic effect on the catalytic decomposition process.

A typical data set for the stoichiometry of the decomposition is shown in Table I. The concentration ratios of the reacted chlorite ion and the products clearly indicate that reaction 1 alone

(13) (a) Sillén, L. G.; Martell, A. E. *Stability Constants*; Chemical Society: London, 1964; Supplement No. 1, 1971. (b) *Stability Constants of Metal-Ion Complexes, Part A: Inorganic Ligands*; Högfeldt, E., Ed.; IUPAC Chemical Data Series No. 21; Pergamon Press: Oxford, U.K., 1982.
(14) Pouli, D.; Smith, W. M. *Can. J. Chem.* **1960**, *38*, 567.
(15) Gordon, G.; Tachiyashiki, S. *Environ. Sci. Technol.* **1991**, *25*, 468.
(16) Tang, T.-F.; Gordon, G. *Environ. Sci. Technol.* **1984**, *18*, 212.
(17) Milburn, R. M.; Vosburgh, W. C. *J. Am. Chem. Soc.* **1955**, *77*, 1352.
(18) Popa, G.; Luca, C.; Iosif, E. *Z. Phys. Chem. (Leipzig)* **1963**, *222*, 49.
(19) Kieffer, R. G.; Gordon, G. *Inorg. Chem.* **1968**, *7*, 239.

is not sufficient to characterize the stoichiometry. This finding is in contradiction with the results of Schmitz and Rooze.[8] Since these authors did not report the details of their experiments, we could not trace the source of the discrepancy. According to our data, only the combination of reactions 1 and 2 can properly describe the observed concentration ratios. In this respect, the catalytic decomposition is analogous to the uncatalyzed reaction. It should be added that the stoichiometry varies slightly with the actual concentrations and it also appears to change to some extent within a given kinetic run.

Typical SF traces at 370 nm are shown in Figure 2. Since neither ClO_2^- nor the catalyst solutions have significant absorbance at 370 nm, the sharp increase at the very beginning of these curves corresponds to the very fast formation of one or more new species. In the first 15–20 ms, the rate of the absorbance change is consistent with the formation of $FeClO_2^{2+}$. However, other species also may contribute to the overall spectral effect. Even with the initial region ignored, the SF traces reflect composite kinetic features. The experimental data could not be interpreted in terms of a simple rate law.

The interplay of various kinetic effects also was observed at 510 nm, where the primary absorbing species[9] is $FeClO_2^{2+}$. The complex formation is rapid, and $FeClO_2^{2+}$ is in pseudoequilibria with chlorite ion. Accordingly, as the decomposition proceeds and the chlorite ion concentration decreases, steadily decaying absorbance curves are expected. At lower chlorite ion concentrations the SF traces were consistent with this expectation. However, the absorbance change was reversed by increasing the initial concentration of ClO_2^-. This observation probably can be interpreted in terms of massive chlorine dioxide formation. ClO_2 is characterized by a very weak absorbance at 510 nm. Still, at high concentration levels, its increasing contribution to the measured absorbance overcompensates the disappearance of the $FeClO_2^{2+}$ complex.

The fast kinetic measurements presented here and reported earlier provide ample kinetic information concerning the initial part of the decomposition reaction. In general, the observed spectral changes reflect simultaneous concentration changes of ClO_2^-, $HClO_2$, ClO_2, $Fe(OH)^{2+}$, $FeClO_2^{2+}$, and possible other iron(III) species. In addition, the equilibria between the corresponding acid–base pairs are continuously repositioned during the reaction, depending on the actual stoichiometry involving the hydrogen ion. In the absence of buffers, this latter problem is eliminated, but additional side reactions, such as complex formation with the buffer, offset this advantage.

In principle, the experimental data can be evaluated by using advanced fitting procedures and the concentration vs time profiles can be calculated for each component. However, considering the complexity of the present system coupled with the experimental limitations, the integrity of the results from such calculations is questionable. For example, among the various components, chlorine dioxide has the most characteristic spectrum and the most reliable concentrations are expected for this species. In this context, preliminary evaluation of the data by using a nonlinear least-squares routine[20] gave somewhat ambiguous concentrations even for ClO_2.

The application of the QSF method offers a possibility of determining the concentration vs time profiles for the reactants and products. This fast kinetic technique was developed primarily for studying biochemical reactions which are not associated with characteristic spectral changes.[21]

The QSF method has not been generally applied in kinetic studies of inorganic reactions. The schematic of the instrument applied in this study is shown in Figure 3. Basically, the QSF method consists of two stopped-flow sequences which are electronically controlled and monitored. First, drive I is activated and the studied reaction is triggered by fast mixing of the reactants in mixer I. By the end of this stage, the reaction tube is filled

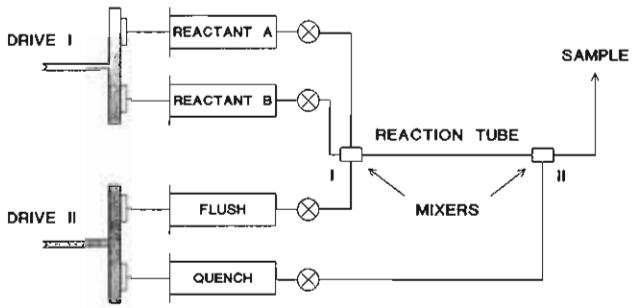

Figure 3. Schematic of the quenched stopped-flow instrument.

with the reaction mixture. After a certain incubation period, drive II is activated. The reaction tube is flushed in order to force the reaction mixture out of the aging tube. Generally, 1.0 M $NaClO_4$ is used in order to reduce the corrupted end-zone of the reaction plug. The flush solution also contains NaF at relatively low concentration levels to quench the catalytic effect of any unreacted iron(III). Immediately following the flush, the reaction is chemically stopped by injecting the quench reagent into the reaction mixture (mixer II). The collected samples can be conveniently analyzed by a variety of techniques.

Providing that the quench reaction is extremely fast, the average age of the quenched reaction mixture (t_a) is given by eq 3, where

$$t_a = V_T(t_I/V_R + t_{II}/V_Q)/2 + t_d \qquad (3)$$

V_T, V_R, V_Q, t_I, t_{II}, and t_d are the volumes of the reaction tube, the delivered reaction mixture, and quench solution, the duration times of drives I and II, and the time delay between the two SF sequences, respectively. In order to obtain uniformly aged samples, the speed of the two drives has to be synchronized such that $t_I/V_R = t_{II}/V_Q$. As a result of a detailed calibration, the reproducibility of the delivered volumes of the reactants and the quench and flush solutions as well as their flow rates is ±1.5%. With the actual configuration, the cumulative dead time (the shortest t_a) was ~40 ms.

In the stoichiometric experiments, fluoride ion effectively stopped the catalytic decomposition of ClO_2^-, and the contribution of fluoro complexes to the measured spectra was negligible. The formation kinetics of the iron(III) monofluoro complex was investigated in 0.02–0.4 M perchloric acid by Pouli and Smith.[14] On the basis of the activation parameters given by these authors, the estimated forward rate constant for the $Fe^{3+} + F^- = FeF^{2+}$ step is 5.4×10^3 M^{-1} s^{-1} at 25 °C. With this rate constant, the calculated lifetime of free iron(III) would be ~3 ms in 0.05 M F^- solution. In less acidic solutions, i.e. at pH >2.0, a much faster complex formation is expected because ligand substitution reactions of iron(III) are much faster[22] via $Fe(OH)^{2+}$ than via Fe^{3+}. Stopped-flow measurements in the Fe^{3+}–F^- system were consistent with this expectation.

The ability of fluoride ion to quench the decomposition was further tested in SF-RS experiments by mixing solutions of ClO_2^- and F^- with iron(III) solution. No chlorine dioxide formation was observed in these experiments, indicating that, for all practical purposes, the catalyst was instantaneously deactivated. Since fluoride ion acts as a buffer ($pK_a = 2.95$[13]) and increases the pH above 2.7, the uncatalyzed decomposition also was stopped. On the basis of these results, fluoride ion was used as quencher in 0.1 M or higher concentrations in the QSF measurements.

In the first set of QSF experiments, the quenched samples were diluted in formate buffer and analyzed as detailed in the Experimental Section. As seen in Table II, the results are consistent with the stoichiometric studies at longer times of the reaction. It should be noted that, in the initial part of the reaction, the experimental error in the chlorite ion determination is comparable with its concentration change. Therefore, only the $[ClO_2]/[Cl^-]$

(20) Fábián, I. Private communication. *NESSIE: A General Purpose Non-Linear Least Square Fitting Program*; Debrecen, Hungary, 1982.
(21) Barman, T. E.; Travers, F. *Methods Biochem. Anal.* **1985**, *31*, 1.
(22) Margerum, D. W.; Cayley, G. R.; Weatherburn, D. C.; Pagenkopf, G. K. In *Coordination Chemistry*; Martell, A. E., Ed.; American Chemical Society: Washington, DC, 1978; Vol. 2, pp 1–220 and references therein.

Table II. Typical Stoichiometric Results from Quenched Stopped-Flow Studies for the Iron(III)-Catalyzed Chlorite Ion Decomposition[a]

time, s	$10^2C_{ClO_2^-}$, M	$10^3C_{ClO_2}$, M	$10^3C_{Cl^-}$, M	C_{ClO_2}/C_{Cl^-}
0.0	10.03			
0.089	10.05	0.63	0.30	2.14
0.188	10.04	1.01	0.42	2.38
0.539	9.91	1.67	0.66	2.53
1.140	9.85	2.36	1.02	2.31
2.037	9.60	3.09	1.26	2.45
3.041	9.60	3.66	1.34	2.75
4.037	9.44	4.19	1.67	2.51
5.042	9.46	4.56	1.65	2.76
6.039	9.40	5.00	1.82	2.65
8.039	9.19	5.59	1.98	2.82
10.038	9.02	5.98	2.17	2.79

[a] Conditions: $C_{ClO_2^-}$ = 0.100 M, $C_{Fe^{3+}} = 8.26 \times 10^{-4}$ M, $C_{HClO_4} = 6.59 \times 10^{-2}$ M; quencher 0.25 M NaF.

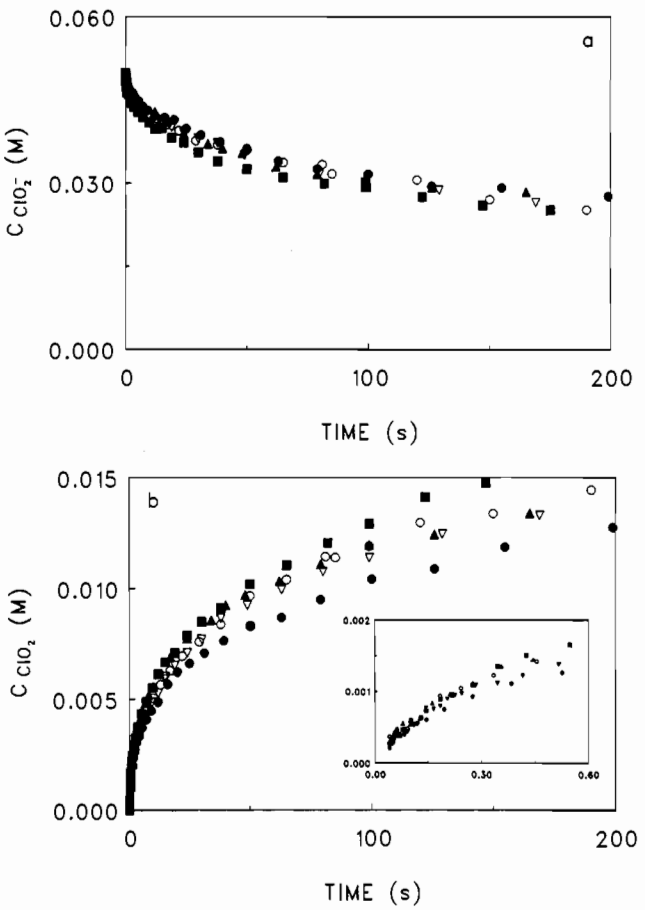

Figure 4. Concentration vs time profiles obtained from the quenched stopped-flow experiments for chlorite ion (a) and chlorine dioxide (b) as a function of the pH. Insert: enlarged first portion of the same curves. $C_{ClO_2^-} = 4.99 \times 10^{-2}$ M and $C_{Fe^{3+}} = 1.39 \times 10^{-3}$ M. pH: 1.25 (●); 1.50 (▽); 1.75 (○); 2.00 (■); 2.25 (▲).

concentration ratio should be considered to be a reliable indicator of the stoichiometry.

Typical kinetic curves are shown in Figures 4 and 5. These figures, as well as Table II, demonstrate that otherwise unavailable quantitative information could be obtained by using the QSF method. Most importantly, the concentration vs time profiles for chlorite ion were obtained directly for the initial part of the reaction.

In agreement with the results from conventional kinetic measurements, the reaction rate exhibits negligible pH dependence in the pH 1.25–2.25 range. The disappearance of chlorite ion and the formation of chlorine dioxide show analogous kinetic patterns in the entire time domain, each indicating the autoinhibitive character of the decomposition. This observation can be rationalized by assuming either the steady removal of the catalytically active iron(III) species or, as suggested by Schmitz and Rooze,[8] a mechanism in which the product ClO_2 inhibits the decomposition. In order to distinguish between the two possibilities, several QSF runs were repeated in an open reactor by continuously purging the reaction mixture with N_2. This method was sufficient to remove substantial amounts of chlorine dioxide, though the efficiency was not quantified. In spite of the semiquantitative nature of these experiments, the comparison of the corresponding conversion data at the same reaction time (Table III) proves that more chlorite ion decomposed in the open reactor; i.e., the inhibition is probably associated with chlorine dioxide formation.

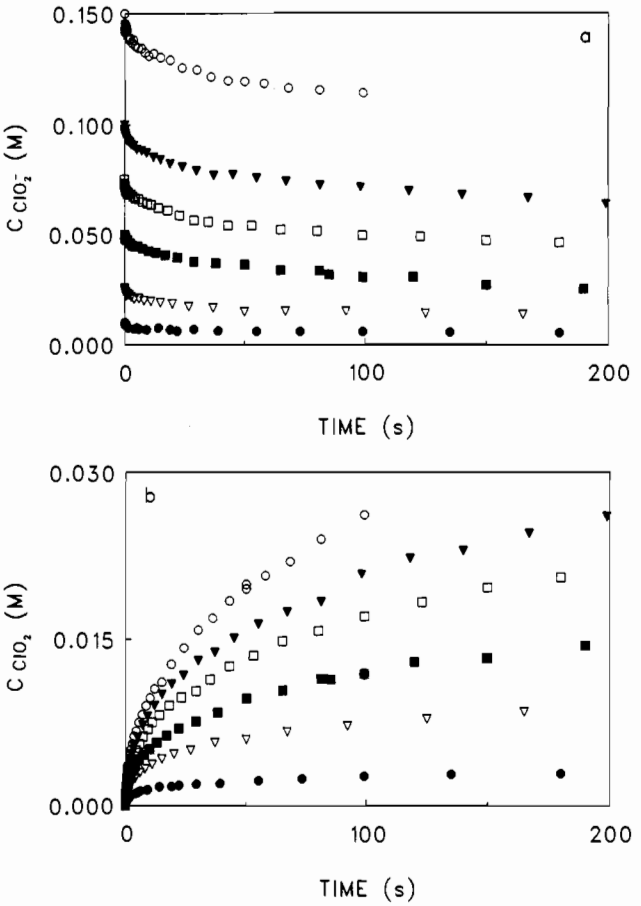

Figure 5. Concentration vs time profiles obtained from the quenched stopped-flow experiments for chlorite ion (a) and chlorine dioxide (b) as a function of the chlorite ion concentration. pH = 1.75 and $C_{Fe^{3+}} = 1.39 \times 10^{-3}$ M. $C_{ClO_2^-}$: 9.99×10^{-3} M (●); 2.50×10^{-2} M (▽); 4.99×10^{-2} M (■); 7.50×10^{-2} M (□); 9.99×10^{-2} M (▼); 0.150 M (○).

Table III. Comparison of Conversions in QSF Experiments and in an Open Reactor after 3-min Reaction Time[a]

		% reacted chlorite ion	
pH	$10^3C_{Fe^{3+}}$, M	QSF exp[b]	open reactor
1.25	1.40	43.3	57.2
1.50	1.40	47.4	63.3
1.75	1.40	48.5	71.6
2.00	1.40	50.0	68.6
1.75	2.79	45.2	79.9
1.75	4.19	54.0	83.6

[a] $C_{ClO_2^-}$ = 0.100 M. [b] Interpolated values.

Discussion

The Mechanism. A detailed kinetic model for the catalytic decomposition of ClO_2^- is summarized in Table IV. As a result of our SF studies, we propose that the catalytic decomposition is initiated by complex formation between chlorite ion and iron(III). The intrinsic mechanism for the $FeClO_2^{2+}$ formation includes fast protolytic equilibria between the corresponding acid–

base pairs and the ligand substitution steps with Fe^{3+} and $Fe(OH)^{2+}$ (the first five reactions in Table IV).[9] The SF experiments also confirmed that the redox decomposition of the $FeClO_2^{2+}$ complex competes with its formation, and the value of 30.1 s^{-1} was estimated for the corresponding first-order rate constant. Two alternatives can be envisioned for the decomposition:

$$FeClO_2^{2+} = Fe(IV) + Cl(II) \quad (4)$$

$$FeClO_2^{2+} = Fe^{2+} + ClO_2 \quad (5)$$

Direct experimental evidence appears to be unattainable to distinguish the two possible pathways. However, reaction 4 can be rejected on the basis of the following arguments.

The $FeClO_2^{2+}$ complex shows intense absorbance in the visible region. Similar to those of other iron(III) complexes, this spectral feature is assigned to a ligand to metal charge-transfer band. Accordingly, one electron of the ligand is partially shifted toward the metal center, making more favorable the decomposition via reaction 5 than that via reaction 4. An analogous internal oxidation–reduction pathway was suggested for the decomposition of the $Co(NH_3)_5ClO_2^{2+}$ complex by Thompson.[23]

The fact that chlorine dioxide was observed in the very early phase of the reaction also suggests that reaction 5 is the main pathway of the decomposition. If $FeClO_2^{2+}$ decomposed by means of reaction 4, chlorine dioxide production would start only in a subsequent step between Cl(II) and presumably chlorite ion. Thus, an incubation period would be expected in the concentration vs time profiles for ClO_2. No such incubation period was observed.

In the presence of strong oxidizing agents, such as chlorite ion or chlorine dioxide, iron(II) is rapidly converted into iron(III). For the oxidation of Fe^{2+} by chlorite ion, the mechanism shown in eqs 6–8 was proposed by Ondrus and Gordon[24] (since the exact

$$Fe^{2+} + ClO_2^- = Fe^{3+} + \{Cl(II)\} \qquad k_7 = 2.0 \times 10^3\ M^{-1}\ s^{-1} \quad (6)$$

$$Fe^{2+} + HClO_2 = Fe^{3+} + \{Cl(II)\} \qquad k_8 = 5.8 \times 10^3\ M^{-1}\ s^{-1} \quad (7)$$

$$\{Cl(II)\} + Fe^{2+} = Fe^{3+} + HOCl \qquad \text{fast} \quad (8)$$

composition of the transient species is not known, these equations were not balanced).

The transient chlorine(II) species is extremely reactive and is in steady state. Thus, a simple two-term second-order rate law, shown in eq 9, can be derived for the overall oxidation process.

$$v = (k_7[ClO_2^-] + k_8[HClO_2])[Fe^{2+}] \quad (9)$$

Under our experimental conditions, chlorite ion is in 10^3–10^4-fold excess over iron(II). In addition, the reactions between ClO_2^- and lower oxidation state chlorine species, with the exception of Cl^-, are generally fast.[11,25] Accordingly, a fast reaction can be envisioned between the chlorine(II) intermediate and chlorite ion (reaction 10) which is superior to reaction 8 and replaces it in the Ondrus–Gordon mechanism.

$$\{Cl(II)\} + ClO_2^- = ClO^- + ClO_2 \quad (10)$$

For the reaction sequence of eqs 6, 7, and 10, the rate law and stoichiometry are given by eqs 9 and 11, respectively. In principle,

$$Fe^{2+} + 2ClO_2^- + 3H^+ = Fe^{3+} + HOCl + ClO_2 + H_2O \quad (11)$$

the product HOCl is in fast acid–base equilibrium with ClO^- ($pK_a \sim 7.5$).[13] However, in the applied pH region, this equilibrium is completely shifted to HOCl and need not be considered in the mechanism.

Iron(II) is also oxidized by the product chlorine dioxide, and as the reaction proceeds, this pathway becomes increasingly significant. The oxidation may occur in a single outer-sphere step or in an inner-sphere process, which implies that reaction 5 is reversible. Since the two alternative pathways are experimentally indistinguishable and give equivalent interpretations of the oxidation, in further discussions only the inner-sphere mechanism will be considered. At this point, it should be emphasized that the forward rate constant for reaction 5 was estimated on the basis of SF experiments in the first 40–50 ms of the overall reaction,[9] where the contribution of ClO_2 to the oxidation of Fe^{2+} is presumably small but not necessarily negligible. Accordingly, the estimated value for k_6 appears to be reliable only within a factor of 2–3.

By using the corresponding standard electrode potentials, Schmitz and Rooze[8] estimated the equilibrium constant between the Fe^{3+}/Fe^{2+} and ClO_2/ClO_2^- redox couples in 1.0 M $NaClO_4$ at 25 °C: $K = [ClO_2][Fe^{2+}]/([ClO_2^-][Fe^{3+}]) = 2.7 \times 10^{-4}$. With this value and the stability constant of the $FeClO_2^{2+}$ complex,[9] K_6 was calculated to be 2.0×10^{-5} M. On the basis of this equilibrium constant and $k_6 = 30.1\ s^{-1}$, $1.5 \times 10^6\ M^{-1}\ s^{-1}$ was obtained for k_{-6}. Obviously, these values are only as good as the equilibrium and kinetic parameters used for their estimation. While the standard electrode potential for the Fe^{3+}/Fe^{2+} couple appears to be well established ($\epsilon^\circ = 0.771$ V), there is certain ambiguity in the value for the ClO_2/ClO_2^- couple. For example, the standard electrode potential used by Schmitz and Rooze[8] ($\epsilon^\circ = 0.935$ V) is 133 mV less than the value recently recommended by Bratsch[26] ($\epsilon^\circ = 1.068$ V). Earlier electrode potentials for the ClO_2/ClO_2^- couple suggest even larger divergence.[27] A 133-mV variation in the electrode potential results in more than 2 orders of magnitude uncertainty in K_6 and k_{-6}.

At longer times, the ClO_2 concentration increases and the oxidation of Fe^{2+} by chlorite ion becomes less important when compared to reaction 5. The chlorine dioxide production slows down, and the system approaches an equilibrium state, which is primarily determined by the complex formation and reaction 5. This interpretation is consistent with the inhibitive feature of the overall reaction. It should be added that, in various redox reactions of oxychlorine species, ClO_2 is one of the final products which does not react with other chlorine species. Therefore, no other chemically acceptable pathway can be envisioned for the chlorine dioxide inhibition in the present system.

Additional steps of the mechanism include the reaction of hypochlorous acid, formed in reaction 11, with chlorite ion. This reaction has been investigated under a variety of experimental conditions.[11,15,16,25,28,29] It is generally agreed that higher reactant concentrations, lower pH, and chlorite ion excess favor the formation of chlorine dioxide over chlorate ion. In acidic solution, the hypochlorous acid–chlorite ion reaction is extremely fast and probably does not become rate determining in the chlorite ion decomposition. As a consequence, hypochlorous acid cannot accumulate in this system and is in steady state. Nevertheless, a precise kinetic model for the $HOCl–ClO_2^-$ reaction is crucial because the final stoichiometry is determined by the delicate balance between the two competing pathways leading to the formation of ClO_2 and ClO_3^-.

With a few modifications, the mechanism proposed by Peintler et al.[11] was adopted for the $HOCl–ClO_2^-$ reaction. Similar to other kinetic models, this mechanism postulates the formation of the reactive Cl_2O_2 intermediate.

$$ClO_2^- + HOCl + H^+ = Cl_2O_2 + H_2O \qquad k = 1.1 \times 10^6\ M^{-2}\ s^{-1} \quad (12)$$

By taking into account the protonation of chlorite ion as a fast preequilibrium, one can rewrite eq 12 in the following form:

$$HClO_2 + HOCl = Cl_2O_2 + H_2O \qquad k_{10} = 2.1 \times 10^4\ M^{-1}\ s^{-1} \quad (13)$$

Rate constant k_{10} is calculated by using $pK_a = 1.72$[12] for chlorous acid.

(23) Thompson, R. C. *Inorg. Chem.* **1979**, *18*, 2379.
(24) Ondrus, M. G.; Gordon, G. *Inorg. Chem.* **1972**, *11*, 985.
(25) Emmenegger, F.; Gordon, G. *Inorg. Chem.* **1967**, *6*, 633.
(26) Bratsch, S. G. *J. Phys. Chem. Ref. Data* **1989**, *18*, 1.
(27) Latimer, W. *Oxidation Potentials*, 2nd ed.; Prentice-Hall: Englewood Cliffs, NJ, 1952.
(28) Taube, H.; Dodgen, H. *J. Am. Chem. Soc.* **1949**, *71*, 3330.
(29) Aieta, E. M.; Roberts, P. V. *Environ. Sci. Technol.* **1986**, *20*, 50.

The following two steps were justified for the Cl_2O_2 intermediate:

$$Cl_2O_2 + ClO_2^- = 2ClO_2 + Cl^- \quad (14)$$

$$Cl_2O_2 + H_2O = ClO_3^- + Cl^- + 2H^+ \quad (15)$$

Although the rates of these reactions have different concentration dependences, the corresponding rate constants could not be determined, only their ratio: $k_{11}/k_{12} = 5.4 \times 10^4$ M^{-1}. The Cl_2O_2 intermediate is presumably in steady state; i.e., reactions 14 and 15 should be considerably faster than reaction 13. In order to obtain this condition, $k_{11} = 5 \times 10^8$ M^{-1} s^{-1} and $k_{12} = 9.3 \times 10^3$ s^{-1} were used for the calculations.

In the reaction between chloride ion and hypochlorous acid, chlorine is formed, which in turn reacts with chlorite ion[11] ($k_{14} = 3.7 \times 10^3$ M^{-1} s^{-1}). For the Cl^-–HOCl step, the rate constants reported by Eigen and Kustin[30] were accepted without modifications.

Peintler et al. also found some evidence for another third-order reaction step and suggested that it occurs via a preequilibrium[11] between ClO_2^- and HOCl:

$$2HOCl + ClO_2^- = ClO_3^- + Cl_2 + H_2O \qquad k = 2.1 \times 10^4\ M^{-2}\ s^{-1} \quad (16)$$

We propose an alternative interpretation of reaction 16, which includes the formation of chlorine monoxide:

$$2HOCl = Cl_2O + H_2O \quad (17)$$

$$Cl_2O + ClO_2^- = ClO_3^- + Cl_2 \quad (18)$$

Although the formation of chlorine monoxide in aqueous solution and an equilibrium constant for reaction 17 were reported by Roth[31] as early as 1929, this species has not been included in previous mechanisms for the HOCl–ClO_2^- reaction. Kinetic studies related to reaction 17 indicated that it is catalyzed by hydrogen ion and acetic acid.[32-34] According to a recent report by Beach and Margerum,[34] the equilibrium constant (K_{15}) and the forward rate constants for the uncatalyzed (k_{15}) and acetic acid catalyzed pathways are 1.15×10^{-2} M^{-1}, 0.12 M^{-1} s^{-1}, and 280 M^{-2} s^{-1}, respectively. The forward rate constant for the hydrogen ion catalyzed pathway[32] (k_{16}) is 3.1 M^{-2} s^{-1}.

The comparison of the rate constants for the oxidation of the $Ni(CN)_4^{2-}$ complex by Cl_2O, Cl_2, and HOCl demonstrated[34] that chlorine monoxide is the most reactive among these species. If this reflects a general trend, chlorine monoxide may have a central role in the HOCl–ClO_2^- reaction.

Under the experimental conditions applied by Peintler et al.,[11] reaction 17 can be regarded as a fast preequilibrium. On the basis of this approximation, rate constant k_{17} is calculated to be 1.8×10^5 M^{-1} s^{-1}.

The mechanism for the HOCl–ClO_2^- reaction is complete with an additional step recently proposed by Gordon and Tachiyashiki:[15]

$$Cl_2O_2 + HOCl = ClO_3^- + Cl_2 + H^+ \quad (19)$$

As a starting point in the calculations, we use the same rate constant for this step as for reaction 11, i.e. $k_{18} = 5 \times 10^8$ M^{-1} s^{-1}.

Calculations. In order to validate the mechanism, concentration vs time profiles were simulated by using a GEAR algorithm[35] based program (ZITA)[36] and compared with the experimental curves. In the first attempt, all reaction steps were included in the calculations with the originally proposed rate constants (set A in Table IV). With this set of data, a consistently smaller than experimentally observed decomposition rate was calculated for the initial part of the reaction. Also, at longer times the chlorine dioxide production was overestimated and the stoichiometry was consistent with reaction 2. Sensitivity analysis of the parameters confirmed that the reactions between various transient species have, at most, marginal kinetic importance, even if they are assumed to be diffusion controlled. Therefore, reactions 17, and as a consequence 18, and 19 were rejected in further calculations.

The rate-determining step in the overall mechanism is the redox decomposition of the $FeClO_2^{2+}$ complex. Thus, the calculated kinetic curves are very sensitive to the actual parameters for reaction 5. Simultaneously increasing k_6 and decreasing K_6 (i.e. increasing k_{-6}) resulted in simulated concentration vs time profiles for the chlorite ion that approached the experimentally observed curves. The calculations, based on systematic variation of the parameters, gave 100 s^{-1} and 1.3×10^{-5} M as the best values for k_6 and K_6, respectively. Modification of these parameters did not affect the stoichiometry of the reaction.

In contrast to chlorine dioxide, chlorate ion is formed only in fast secondary steps between various chlorine species. Thus, the only possible way to resolve the discrepancy between the measured and calculated stoichiometries is to modify the intrinsic rate constants for the ClO_2^-–HOCl reaction. This would require that the value for the k_{11}/k_{12} ratio be about 3 orders of magnitude smaller. The literature value for k_{11}/k_{12} (5.4×10^4 M^{-1}) was calculated[11] without rigorous confirmation of the stoichiometry by fitting the concentration vs time profiles for chlorine dioxide in the ClO_2^-–HOCl reaction. Simulated kinetic curves calculated

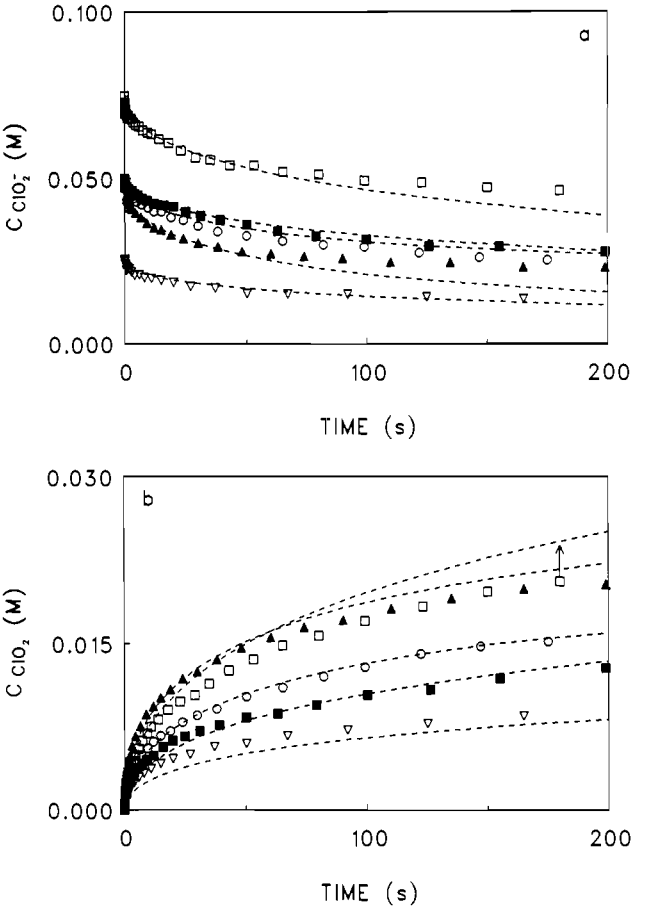

Figure 6. Comparison of a few experimental and simulated (dashed lines) kinetic curves for chlorite ion (a) and chlorine dioxide (b): $C_{ClO_2^-} = 4.99 \times 10^{-2}$ M, $C_{Fe^{3+}} = 1.39 \times 10^{-3}$ M. pH = 1.25 (■); $C_{ClO_2^-} = 4.99 \times 10^{-2}$ M, $C_{Fe^{3+}} = 1.39 \times 10^{-3}$ M, pH = 2.00 (○); $C_{ClO_2^-} = 5.00 \times 10^{-2}$ M, $C_{Fe^{3+}} = 4.20 \times 10^{-3}$ M, pH = 1.75 (▲); $C_{ClO_2^-} = 2.50 \times 10^{-2}$ M, $C_{Fe^{3+}} = 1.39 \times 10^{-3}$ M, pH = 1.75 (▽); $C_{ClO_2^-} = 7.50 \times 10^{-2}$ M, $C_{Fe^{3+}} = 1.39 \times 10^{-3}$ M, pH = 1.75 (□).

(30) Eigen, M.; Kustin, K. *J. Am. Chem. Soc.* **1962**, *84*, 1355.
(31) Roth, W. A. *Z. Phys. Chem., Abt. A* **1929**, *145*, 289.
(32) Swain, C. G.; Crist, D. R. *J. Am. Chem. Soc.* **1972**, *94*, 3195.
(33) Israel, G. C. *J. Chem. Soc.* **1950**, 1286.
(34) Beach, M. W.; Margerum, D. W. *Inorg. Chem.* **1990**, *29*, 1225.
(35) Hindmarsh, A. C. *GEAR: Ordinary Differential Equation Solver.* Technical Report No. UCM-3001, Revision 2; Lawrence Livermore Laboratory; Livermore, CA, 1972.
(36) Peintler, G. Private communication. *ZITA 2.1, a software package for simulating and fitting kinetic curves*; Szeged, Hungary, 1991.

Table IV. Proposed Mechanism for the Iron(III)-Catalyzed Decomposition of Chlorite Ion

reaction	rate constant[a]	set A	ref[b]	set B[c]
Complex Formation				
$H^+ + ClO_2^- = HClO_2$		fast equil		
$K_1 = 52.5\ M^{-1}$				
$Fe^{3+} = Fe(OH)^{2+} + H^+$		fast equil		
$K_2 = 1.82 \times 10^{-3}\ M$				
$Fe^{3+} + ClO_2^- = FeClO_2^{2+}$	k_3	2.7×10^2	10	2.7×10^2
$K_3 = 13.8\ M^{-1}$	k_{-3}	19.5	10	19.5
$Fe(OH)^{2+} + ClO_2^- = Fe(OH)ClO_2^+$	k_4	5.0×10^3	10	5.0×10^3
$K_4K_5 = 7.6 \times 10^3\ M^{-2}$	k_{-4}/K_5	0.66	10	0.66
$Fe(OH)ClO_2^+ + H^+ = FeClO_2^{2+}$		fast equil		
$K_4K_5 = 7.6 \times 10^3\ M^{-2}$				
Decomposition of the $FeClO_2^{2+}$ Complex				
$FeClO_2^{2+} = Fe^{2+} + ClO_2$	k_6	30.1	10	100
$K_6 = 2.0 \times 10^{-5}\ M$	k_{-6}	1.5×10^6	9	7.6×10^6
Oxidation of Fe^{2+}				
$Fe^{2+} + ClO_2^- \rightarrow Fe^{3+} + Cl(II)$	k_7	1.9×10^3	24	1.9×10^3
$Fe^{2+} + HClO_2 \rightarrow Fe^{3+} + Cl(II)$	k_8	3.0×10^3	24	3.0×10^3
$ClO_2^- + Cl(II) \rightarrow HOCl + ClO_2$		very fast		
Reactions of Chlorine Species				
$HOCl + HClO_2 = Cl_2O_2 + H_2O$	k_{10}	2.1×10^4	11	2.1×10^4
$Cl_2O_2 + ClO_2^- = 2ClO_2 + Cl^-$	k_{11}[d]	5.0×10^8	11	5.0×10^8
$Cl_2O_2\ (+H_2O) = ClO_3^- + Cl^- + 2H^+$	k_{12}[d]	9.3×10^3	11	1.0×10^7
$HOCl + Cl^- + H^+ = Cl_2\ (+H_2O)$	k_{13}	1.8×10^4	30	1.8×10^4
$K_{13} = 1.7 \times 10^3\ M^{-2}$	k_{-13}	11	30	1.1×10
$Cl_2 + ClO_2^- = Cl_2O_2 + Cl^-$	k_{14}	3.7×10^3	11	3.7×10^3
$2HOCl = Cl_2O\ (+H_2O)$	k_{15}	0.12	34	
$K_{15} = 1.15 \times 10^{-2}\ M^{-1}$	k_{-15}	11	34	
$2HOCl + H^+ = Cl_2O + H^+\ (+H_2O)$	k_{16}	3.1	32	
$K_{16} = K_{15}$	k_{-16}	2.7×10^2	32	
$Cl_2O + ClO_2^- = ClO_3^- + Cl_2$	k_{17}	1.8×10^5	*e*	
$Cl_2O_2 + HOCl = ClO_3^- + Cl_2 + H^+$	k_{18}	5.0×10^8	*e*	

[a] First-, second-, and third-order rate constants are in s^{-1}, $M^{-1}\ s^{-1}$, and $M^{-2}\ s^{-1}$, respectively. [b] The rate constants in set A were directly obtained from or estimated on the basis of the corresponding reference. [c] See text. [d] According to ref 11, $k_{11}/k_{12} = 5.4 \times 10^4\ M^{-1}$. [e] Estimated in this work.

on the basis of the modified set of rate constants (set B, Table IV) correlate excellently with the experimental results. Examples are shown in Figure 6.

At longer reaction times and at higher pH values and chlorite ion and iron(III) concentrations, the calculations tend to predict faster than observed decomposition. This finding strongly suggests that the inclusion of additional steps may be necessary to obtain a more precise mechanism for the decomposition.

Theoretically, a better data set could be obtained for the rate constants by combining the simulations with a nonlinear least-squares fitting procedure as is described in detail elsewhere.[11] However, a meaningful fitting procedure will require more reliable parameters for several independent steps of the mechanism, such as the rate constants of the $HOCl-ClO_2^-$ reaction and the equilibrium constant for reaction 5. Because of the lack of these data, which necessarily must be obtained from independent studies, no further attempt was made to optimize the kinetic model.

Conclusions. The application of a variety of fast kinetic techniques made it possible to explore the initial part of the iron(III)-catalyzed chlorite ion decomposition. It was demonstrated that the QSF method can successfully be used for studying inorganic reactions. The main advantage of this method over other fast kinetic techniques is that the samples can be analyzed by using conventional analytical procedures and the concentration vs time profiles are readily obtained for the reactants and products. The cumulative dead time is about 1 order of magnitude higher than it is with the SF method. However, this disadvantage is partly offset by the fact that the same rate constants can be determined by using lower initial reactant concentrations. This is because pseudo-first-order conditions do not have to be maintained during the kinetic runs.

In spite of the obvious advantages, the QSF method cannot substitute completely for other fast kinetic techniques because it is not suitable for the detection and identification of reactive transient species. Therefore, the QSF, SF, and SF-RS methods should be considered as complementary techniques which together may provide comprehensive kinetic information for a wide variety of reactions.

The kinetic model obtained for the decomposition of chlorite ion gives a reasonable description of the reaction rate and stoichiometry. It was confirmed that the precursor in this mechanism is the $FeClO_2^{2+}$ complex and the rate-determining step is its redox decomposition. Although the calculations indicated that additional steps may have some effect on the reaction, we believe that all kinetically significant steps have been included in the mechanism for the conditions applied in this study. In other words, the mechanism proposed corresponds to the minimum basis set of reactions. However, it should be emphasized that if the experimental conditions are significantly different from those reported here, the mechanism may prove to be incomplete, requiring the postulation of other reaction steps.

On the basis of the mechanism, the possible effects of iron impurities on the reactions of chlorite ion can be estimated. For example, in the presence of 10^{-6} M iron(III) and at pH ~2.0, 2–4% of the chlorite ion decomposes in about 5 min, after which the decomposition practically stops. In terms of stoichiometry, this concentration change may be negligible, but the kinetic role of the transient species formed in the catalytic reaction may be significant. Also, in open reaction systems, which allow the loss of chlorine dioxide, the effects of the decomposition may be more pronounced. The results indicate that impurities may significantly alter the reactions of chlorite ion even at very low concentration levels.

Acknowledgment. We thank Mr. Gábor Peintler of Szeged, Hungary, for the actual version of the program ZITA used in the calculations. We also express our gratitude to Merrell Dow Chemicals (Cincinnati, OH) for lending us the quenched stopped-flow instrument.

Registry No. ClO_2^-, 14998-27-7; Fe, 7439-89-6.